UV–Vis Absorption Spectroscopy of Polonium(IV) Chloride Complexes: An Electronic Structure Theory Study

Ange Stoïanov, Julie Champion, Rémi Maurice

UV-Vis Absorption Spectroscopy of Polonium(IV) Chloride Complexes: An Electronic Structure Theory Study

Ange Stoïanov, Julie Champion, and Rémi Maurice*

SUBATECH, UMR CNRS 6457, IN2P3/IMT Atlantique/Université de Nantes, 4 rue Alfred Kastler, BP 20722, 44307 Nantes Cedex 3, France

E-mail: remi.maurice@subatech.in2p3.fr

Date of preparation: April 23, 2019.

Prepared for *Inorg. Chem.*

Abstract

More than a hundred years after its discovery, the chemistry of the polonium radioelement is still largely unknown. However, it is quite clear that the properties of this heavy element ($Z = 84$) may be affected by relativistic effects, in particular scalar relativistic effects and the so-called spin-orbit coupling (SOC). In this article, we revisit the interpretation of UV-Vis absorption spectra of polonium(IV) complexes in HCl medium, reported decades ago. From the data, two complexes were hypothesized, complex I with a maximum of absorption at 344 nm (at low HCl concentration) and complex II with a maximum at 418 nm (the only visible peak for HCl concentrations above 0.5M). By monitoring the absorbance at 344 and 418 nm as a function of both the HCl concentration and the pH, complex I was formulated as $[Po(OH)Cl_x]^{3-x}$ while complex II was as $[PoCl_{2+x}]^{2-x}$. In this work, we study the ground-state geometries of the $[Po(OH)Cl_x]^{3-x}$ and $[PoCl_{2+x}]^{2-x}$ complexes for $x = 4$–2, *i.e.* for the most probable complexes, with DFT, demonstrating that solvation can remarkably change the geometries of such systems. The electronic excitation energies are then computed with TD-DFT, NEVPT2 and c-SOCI, showing (i) that the SOC must be at play to obtain excitation energies in the right energy domain and (ii) that the quantum chemical calculations point toward $x = 4$, *i.e.* toward the $[Po(OH)Cl_4]^-$ and $[PoCl_6]^{2-}$ complexes.

1 Introduction

The chemistry of the polonium radioelement ($Z = 84$) remains largelly unexplored[1,2] despite its early discovery in 1898 by Marie and Pierre Curie. This radioelement is naturally present in environment.[3] Thus, humans are *de facto* exposed to its radiation, in particular to the polonium-210 ones. Also, anthropic activities may modify local polonium concentrations, for instance in tobacco leaves (phosphate fertilizers)[4] or in coal ashes (thermic power plants).[5]

At the atomistic or molecular level, little structural information is experimentally known. The first ionization potential (IP) of the free atom, already estimated by Charles in 1966 to 8.417 eV,[6] has been very recently redetermined by means of two independent experiments,[7,8] TRIUMF ISAC and CERN ISOLDE, leading to an average value of 8.41807 eV. Such forefront experiments are of invaluable interest for computational chemists, since they lead to reference values for testing the most accurate methodologies as well as more approximate ones. For instance, Borschevsky *et al.*[9] proposed a reference computational value of 8.432 eV for this IP (by means of fully relativistic calculations plus Breit and quantum electrodynamics corrections), as well as a series of more approximate ones. The situation is much less clear regarding the chemical behavior of polonium species in solution. Notably, the complexation of the polonium(IV) ion with four distinct ligands has been recently studied by one of us.[10] However, due to the lack of a firm argument concerning the identification the starting species, so far only apparent constants have been defined from the speciation change studies (performed by monitoring the radioactivity distribution).

In this context, our objective is to determine a "zero point" for studying polonium speciation changes in solution by firmly identifying at least one chemical species of polonium, obviously under known experimental conditions. In this work, we report a first attempt toward this by providing new arguments concerning the polonium speciation based on new quantum mechanical calculations. In particular, we will base our analysis on the confrontation of new computational results to old UV-Vis absorption data obtained in HCl medium.[11] In this seminal study, two polonium(IV) complexes were hypothesized, characterized by maxima of absorption at 344 nm and 418 nm, respectively. While the peak belonging to the former complex was seen for low HCl concentrations, the peak corresponding to the latter complex ended up to be the only visible one for concentrations above 0.5 M. Moyer notably concluded that "at least two complexes involving polonium and chloride ions exist in hydrochloric acid", and by variation of the HCl concentration and of the pH, that the absorption peaks at 344 and 418 nm would correspond to the $[Po(OH)Cl_x]^{3-x}$ and $[PoCl_{2+x}]^{2-x}$ species, respectively,

with x unknown.[11] Because several studies are consistent with the formation of the $[PoCl_6]^{2-}$ complex at high HCl concentrations,[12–16] we first hypothesize that $x \leq 4$. Furthermore, it seems unreasonable to us to consider an x value of 1, since at high HCl concentrations we simply expect that a cationic $[PoCl_3]^+$ species would further interact with chloride ions to form at least the neutral $PoCl_4$ species. By a same reasoning, we also discard the $x = 0$ value. Therefore, we only retain the $x = 4$, 3 and 2 values for this quantum mechanical study, *i.e.* the $[PoOHCl_4]^-/[PoCl_6]^{2-}$, $PoOHCl_3/[PoCl_5]^-$ and $[PoOHCl_2]^+/PoCl_4$ couples.

Within the static quantum mechanical approach (by opposition to the molecular dynamics one), a first shot for modeling maxima of absorption consists in computing vertical electronic excitation energies, leaving aside the vibrational degrees of freedom. Since electron correlation, relativistic effects, and environment effects are susceptible to affect the computed excitation energies, the computational strategy to be employed must by some means account for these physical effects. Polonium(IV) ions are characterized by a formal $[...]6s^2$ atomic electronic structure. Thus, the spin-orbit coupling is expected to hardly affect the molecular geometries of the solvated ions and of the coordination complexes that may form (little population of the $6p$ shell is expected by electron donation from the solvent molecules and/or the ligands by non-covalent interactions and formation of coordination bonds, respectively). Because of this, we will only report scalar-relativistic density functional theory (DFT) optimized geometries, obtained in the absence or in the presence of a conductor-like polarizable continuum model (C-PCM).[17] At the resulting geometries, single-point time-dependent density functional theory (TD-DFT), second-order N-electron valence state perturbation theory (NEVPT2)[18] and contracted spin-orbit configuration interaction (c-SOCI) results will be presented. At the TD-DFT level, the "direct" influence of solvation on the "electronic" excitation energies will be probed at the "gas phase" and at the solvated geometries. Note that the NEVPT2/c-SOCI approach can be quite successful for computing non-adiabatic or vertical energy differences of bound $6p$ systems,[19–23] the missing spin-orbit polarization being more important for describing free atoms/ions and thus dissociation energies.[21,24]

2 Methodology

2.1 Ground-State Geometry Optimizations

Ground-state DFT geometry optimizations have been performed at the SR level within the spin-restricted closed-shell formalism (RDFT, $\langle S^2 \rangle = 0$) with the Gaussian 09 program package.[25] Several starting geometries, corresponding to different molecular symmetry point groups (SPGs), have been considered in each case. For all the converged structures, the absence of any imaginary frequency has been first checked. In most of the cases, only one stable structure has been found. When two stable structures were obtained, the energy difference between the two stable structures has always been more than 10 kJ·mol^{-1}, apart from specific cases that will be detailed in the main text. In each case, only the lowest-energy structure has been reported and retained for the further excitation-energy computations. The B3LYP exchange-correlation functional[26–28] was used, together with the aug-cc-pVTZ[29–31] (H, O and Cl atoms) and the aug-cc-pVTZ-PP[32] (Po atom) basis sets, the latter being used in conjunction with the ECP60MDF energy-consistent pseudopotential.[32] The B3LYP functional was chosen not only due to its widespread use in the literature but also for its observed good performance as compared to CCSD(T) calculations for computing the geometries of hydrated polonium(IV) species.[33]

Two sets of optimized geometries have been collected, namely the "gas phase" (GP) one, actually corresponding to calculations in vacuum, and the "condensed phase" (CP) one, actually corresponding to calculations in vacuum plus the application of a C-PCM perturbation,[17] here meant to implicitly account for solvation effects in water (*i.e.* in aqueous solution). The *alpha* parameter, which is a multiplication factor that is applied to the atom radii prior to building the molecular cavity surface, has been manually set to the 1.2 value. The following radii have been considered: 2.354 Å for Po[34] (as in previous studies by Ayala *et al.*[33,35–37]), 1.980 Å for Cl[38] and 1.520 Å for O.[34] No radius has been applied for the H atom (united atom fashion[38]). Note that a full discussion on the choice of the radii, in particular

the one of the Po atom, is out of the scope of the present work. Actually, test calculations have shown that little structural changes were observed by considering alternative choices of radii, in particular regarding the Po atom, which is quite in a "central" position in the considered complexes (*vide infra*).

2.2 Excitation-Energy Computations

Two sets of excitation-energy computations have been determined. In the first set, spin-orbit free (SOF) excitation energies have been computed by means of TD-DFT,[39] at both the GP and CP geometries, in the absence or in the presence of the C-PCM, with the same computational parameters as for the geometry optimizations (*vide supra*). The TD-DFT solutions consist in linear combinations of single-excited configurations (with respect to the ground configuration). These solutions are by construction mutually orthogonal for each set of given spin "symmetry" (here $\langle S^2 \rangle = 0$ or $\langle S^2 \rangle = 2$) and the outcome of the calculation may slightly depend on the number of roots that is asked for. The number of roots has been set to 3 in each spin subspace to describe only the lowest-lying excited states, in accord with the following WFT study (*vide infra*). These calculations have been performed to highlight the role of the implicit solvation on the SOF excitation energies at both sets of GP and CP geometries. The spin-orbit coupling (SOC) has not been considered in this TD-DFT study, unlike in the complementary and conclusive wave function theory (WFT) one. Of course, only the excitations to spin-singlet states display non-zero oscillator strengths.

Multiconfigurational *and* relativistic WFT calculations have been then performed at the GP and CP geometries with the ORCA program.[40] The "direct" role of solvation on the excitation energies has been neglected. The WFT calculations consists in state-average complete-active space self-consistent field (SA-CASSCF),[41,42] NEVPT2[18] and c-SOCI calculations. Note that NEVPT2 makes use of the so-called Dyall's Hamiltonian,[43] which is meant to prevent the occurrence of spurious intruder states. In the c-SOCI calculations, the SA-CASSCF solutions are used to compute the (offdiagonal) SOC matrix elements, while

the diagonal of the $\mathbf{H}_{\text{total}} = \mathbf{H}_{\text{electronic}} + \mathbf{H}_{\text{SOC}}$ matrix has been dressed with the NEVPT2 "electronic" energies.[44,45] Note that since this matrix is computed within the basis of the SA-CASSCF solutions, $\mathbf{H}_{\text{electronic}}$ is by construction diagonal. Scalar relativistic effects have been explicitly accounted for via the use of the Douglas-Kroll-Hess Hamiltonian.[46–48] The SOC is computed within the mean-field approximation.[49,50] The minimal active space, which consists in 2 electrons within 4 orbitals (*i.e.* an "occupied" MO displaying some $6s$ character and the three "unoccupied" ones displaying strong $6p$ characters), has been used for all the reported results. Test calculations revealed that extension of the active space size was hardly affecting the computed electronic-excitation energies. Naturally, since the DKH Hamiltonian is used, all-electron basis sets had to be employed, unlike in the DFT study. Actually, the SARC-TZVP-DKH basis sets[51,52] have been used for all the atoms. The number of states has been fixed to 4 spin-singlet and 3 spin-triplet states in the SA-CASSCF and thus in the NEVPT2 calculations. Thus, the c-SOCI calculations have resulted in 13 energy levels. Test calculations performed with 10 spin-singlet and 6 spin-triplet SOF states (*i.e.* all the SOF states belonging to the active space) evidenced little effect of the number of SOF on the computed lowest-lying excitation energies.

3 Results and Discussion

3.1 Ground-State Geometry Optimizations

3.1.1 Gas-Phase Geometries

Representations of the gas phase structures are given in Figure 1. Perhaps the first and most important feature to be discussed for a given geometry is its associated molecular SPG. While $[PoCl_6]^{2-}$ and $[PoCl_5]^-$ display trivial SPGs (O_h and D_{3h}, respectively), the symmetry of the other species in the gas phase are a bit less trivial: $PoCl_4$ is a distorted tetrahedron of C_{2v} symmetry, $[Po(OH)Cl_4]^-$ and $[Po(OH)Cl_2]^+$ bear a planar symmetry (C_s SPG), while

$Po(OH)Cl_3$ is hermetic to any symmetry property (C_1 SPG). The full atomic coordinates are given in Section SII. However, one may list here the most important characteristics of these structures, *i.e.* the Po–X bond distances: 2.67 Å for $[PoCl_6]^{2-}$, 2.58 (×3) and 2.61 (×2) Å for $[PoCl_5]^{-}$, 2.58 (×2) and 2.45 (×2) Å for $PoCl_4$, 2.63 (×2), 2.65, 2.58 and 2.06 Å for $[Po(OH)Cl_4]^{-}$, 2.58, 2.53, 2.45 and 2.03 Å for $Po(OH)Cl_3$, and 2.39 (×2) and 2.01 Å for $[Po(OH)Cl_2]^{+}$. In the case of $PoCl_4$, we note that the tetrahedral structure is also a stable one, and that it is quite close in energy to the reported one (*ca.* 2 kJ·mol^{-1} of energy difference in the gas phase).

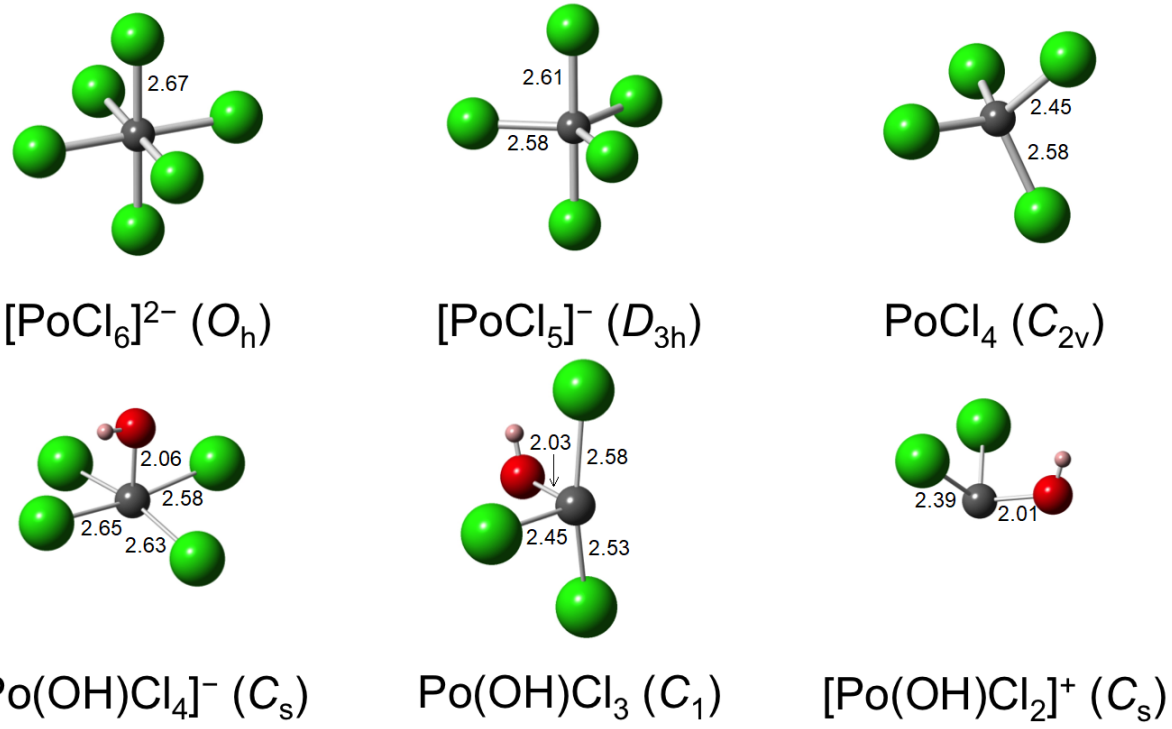

Figure 1: Ball and stick representations of the DFT gas-phase geometrical structures of the $[PoCl_{2+x}]^{2-x}$ (top) and $[Po(OH)Cl_x]^{3-x}$ (bottom) complexes (x = 4–2). Symmetry point groups are indicated in parentheses. Color code: gray stands for Po, green for Cl, red for O, and light pink for H. Bond distances are given in Å.

3.1.2 Condensed-Phase Geometries

As can be seen in Figure 2, important changes on the molecular geometries and in particular on the immediate atomic environment of polonium(IV) ions may be triggered by solvation.

In particular, the structure of $[PoCl_5]^-$ in the presence of the C-PCM perturbation changes to an almost perfect square pyramid (C_{4v} SPG), while the one of $PoCl_4$ becomes much more distorted, being closer to a perfect "seesaw" (disphenoidal geometry of C_{2v} symmetry). Although these geometries may seem quite peculiar for a tetravalent ion, similar geometries have already been reported by Ayala *et al.* for the $[Po(H_2O)_n]^{4+}$ (n = 5, 4) hydrated clusters, which were rationalized in terms of bond analyses and point charge calculations.[33] As previously, the full atomic coordinates are given in Section SII. In these structures, the Po–X bond distances are: 2.65 Å for $[PoCl_6]^{2-}$, 2.62 (×4) and 2.47 Å for $[PoCl_5]^-$, 2.57 (×2) and 2.43 (×2) Å for $PoCl_4$, 2.63 (×2), 2.62, 2.61 and 2.05 Å for $[Po(OH)Cl_4]^-$, 2.58, 2.56, 2.45 and 2.02 Å for $Po(OH)Cl_3$, and 2.40 (×2) and 1.99 Å for $[Po(OH)Cl_2]^+$. Thus, apart from the special case of $[PoCl_5]^-$ for which one bond distance is significantly shortened (which is associated with a SPG change concomitant to quite a significant change in the "apical" ligand field), all the reported distances are affected by less than 0.05 Å upon solvation, meaning that here, only moderate effects on the bond distances are overall observed. In the case of $[PoCl_5]^-$, we note that the trigonal bipyramid structure is also a stable one, and that it is somehow quite close in energy to the reported one (*ca.* 4 kJ·mol^{-1} of energy difference in the condensed phase). Thus, the symmetric D_{3h} structure for $[PoCl_5]^-$ is always a minimum on the potential energy surface (it is a global minimum in the gas phase and a local one in the condensed one). Therefore, the pseudo-Jahn–Teller effect[53] is inactive in both the phases. While for $PoCl_4$ this effect is also inactive in the gas phase (the T_d structure being the global minimum), it may not be the case in the condensed one (the symmetric structure becoming a third-order saddle point). Therefore, the occurrence of a "seesaw" structure in the condensed phase for $PoCl_4$ may be indicative of a solvation-activated pseudo-Jahn–Teller effect. In the remainder of the article, both sets of GP and CP structures will be considered for performing the single-point TD-DFT, NEVPT2 and c-SOCI calculations.

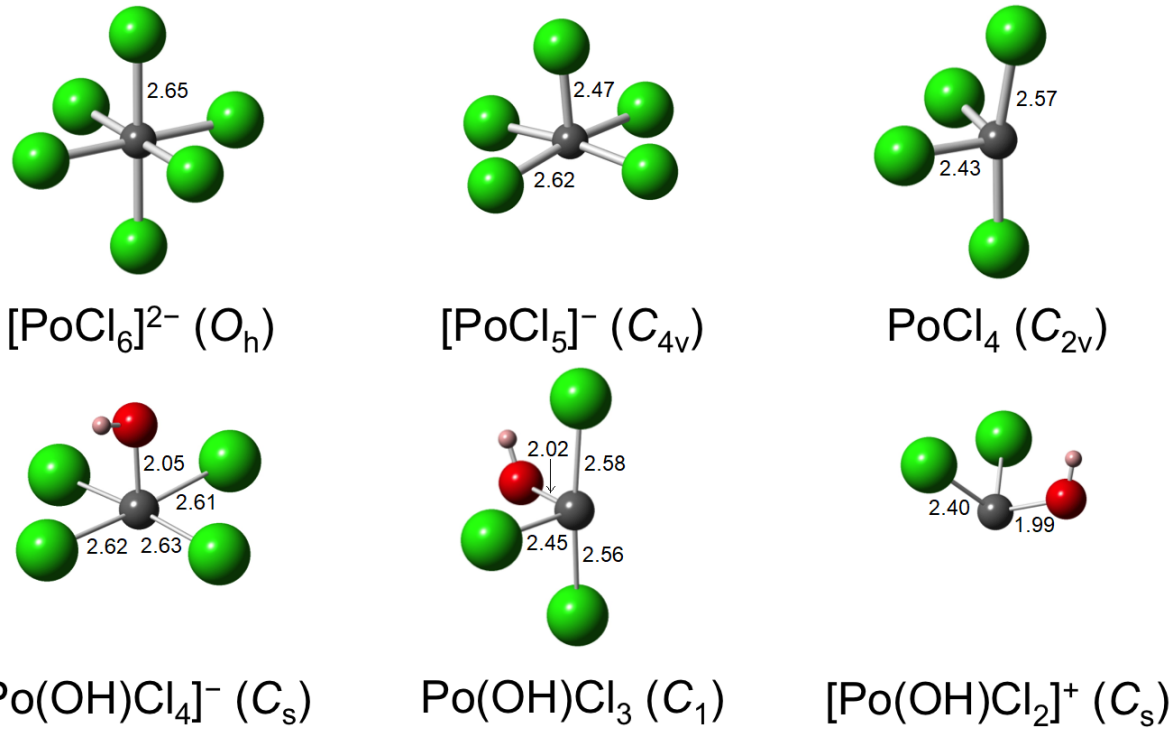

Figure 2: Ball and stick representations of the DFT condensed-phase geometrical structures of the $[PoCl_{2+x}]^{2-x}$ (top) and $[Po(OH)Cl_x]^{3-x}$ (bottom) complexes (x = 4–2). Symmetry point groups are indicated in parentheses. Color code: gray stands for Po, green for Cl, red for O, and light pink for H. Bond distances are given in Å.

3.2 Excitation-Energy Computations

3.2.1 Gas-Phase and Condensed-Phase TD-DFT Excitation Energies

Since not much reference data is available for excitation energies in polonium(IV) complexes, no benchmark study has been devoted to the computation of such quantities by means of TD-DFT, in particular with respect to the choice of the exchange-correlation functional. In this work, we only report a preliminary study aiming at estimating the consequence of (i) the choice of the reference geometry (GP *vs.* CP in Table 1) and (ii) the introduction of the C-PCM perturbation of the excitation energies of interest (GP *vs.* CP = GP + C-PCM in Table 1). Naturally, we expect the following WFT study to provide us with more accurate excitation energies, though these will be generated in the absence of the C-PCM perturbation.

As can be seen in Table 1, apart from the $[PoCl_5]^-$ case which deserves a more detailed discussion, it is clear that the choice of the reference geometries can affect a given computed excitation energy by up to ∼0.5 eV ($PoCl_4$, see in particular the excitation to spin-singlet SOF states). Also, since we have already pointed out that the introduction of the C-PCM can lead to important geometrical changes in polonium(IV) structures, we conclude that it is crucial for the scope of the present study to consider the CP structures for single-point calculations aiming at interpreting the UV-Vis data reported by Moyer.[11] The case of the $[PoCl_5]^-$ complex is more subtle: by going from the D_{3h} (GP) structure to C_{4v} (CP) one, one expects to flip the doubly degenerate spin-singlet and spin-triplet states with the non-degenerate ones (excitation to the $6p_{x,y}$ and $6p_z$ orbitals, respectively). However, since other non degenerate states appear in the spectra (see Table 1), the resulting TD-DFT spectra at the CP geometry are thus qualitatively different from the ones obtained at the GP geometry, *i.e.* they do not correspond to the sole single excitation to the $6p$ orbitals. Note that the expected pattern, *i.e.* one non degenerate and then one doubly degenerate SOF state for each spin "symmetry", will be obtained at the NEVPT2 level (*vide infra*).

As soon as the geometry type (either GP or CP) is fixed, the role of the C-PCM

perturbation on the excitation energies of interest remain moderate: it is always less than ∼0.3 eV for a given excitation energy, and usually no real differential effect between the spin-singlet and spin-triplet states is observed. As will be shown in Section 3.2.2, a key ingredient for describing the UV-Vis spectra reported by Moyer[11] relates to the mixing between the spin-singlet SOF states and some components of the spin-triplet ones spectrum. This mixing relates to the spin-singlet/spin-triplet energy gap(s), and thus, a more important feature of Table 1 is that the C-PCM perturbation does not affect much the gap(s). In other words, it is not crucial to consider the C-PCM perturbation while computing the CP excitation energies. Thus, the following WFT study will be performed only in the gas phase.

Table 1: TD-DFT Excitation Energies (in eV) as Functions of the Geometry and of the Considered Phase. The Numbers of Degenerate Components Are Given in Parentheses, When Relevant.

		GP		CP = GP + C-PCM	
Species	Geometry	$\Delta E(S_0 \rightarrow T_{1-3})$	$\Delta E(S_0 \rightarrow S_{1-3})$	$\Delta E(S_0 \rightarrow T_{1-3})$	$\Delta E(S_0 \rightarrow S_{1-3})$
$[PoCl_6]^{2-}$	GP = O_h	3.69(3)	4.30(3)	3.70(3)	4.36(3)
	CP = O_h	3.76(3)	4.38(3)	3.77(3)	4.43(3)
$[PoCl_5]^-$	GP = D_{3h}	3.13(2); 3.71	3.96(2); 3.97	3.15(2); 3.79	4.05(2); 4.07
	CP = C_{4v}	2.77; 3.17; 3.47[a]	3.13; 3.23; 3.63[a]	2.90; 3.37; 3.61[a]	3.26; 3.42; 3.82[a]
$PoCl_4$	GP = C_{2v}	2.75; 3.03; 3.32	3.70; 3.85; 4.04	2.80; 3.08; 3.38	3.70; 3.88; 4.08
	CP = C_{2v}	2.94; 3.09; 3.33	3.24; 3.43; 3.51	3.13; 3.28; 3.53	3.44; 3.63; 3.71
$[Po(OH)Cl_4]^-$	GP = C_s	3.74; 4.01; 4.03	4.09; 4.26; 4.57	3.97; 4.08; 4.08	4.35; 4.57; 4.77
	CP = C_s	3.75; 4.04; 4.07	4.07; 4.18; 4.53	3.97; 4.10; 4.11	4.32; 4.49; 4.77
$Po(OH)Cl_3$	GP = C_1	3.29; 3.79; 3.96	3.71; 4.06; 4.13	3.44; 3.97; 4.12	3.88; 4.20; 4.28
	CP = C_1	3.26; 3.59; 3.82	3.61; 3.90; 3.93	3.45; 3.83; 4.06	3.82; 4.14; 4.17
$[Po(OH)Cl_2]^+$	GP = C_s	3.97; 4.09; 4.13	4.57; 4.67; 4.68	4.15; 4.20; 4.25	4.67; 4.76; 4.81
	CP = C_s	3.89; 4.04; 4.05	4.50; 4.59; 4.61	4.09; 4.17; 4.19	4.62; 4.72; 4.73

[a]Extension of the number of requested roots revealed that these solutions are in fact doubly degenerate.

3.2.2 Gas-Phase NEVPT2 and c-SOCI Excitation Energies

To first highlight the importance of the SOC on the potentially active electronic transitions, we will first discuss the case of the $[PoCl_6]^{2-}$ complex. At both GP and CP geometries, this system displays an O_h SPG. The single excitation to the $6p$ levels thus result in one triply degenerate spin-triplet SOF state and one triply degenerate spin-singlet one (see Figure 3 and Table 2). Consequently, only one transition is active at the SOF level (red arrow in

Figure 3). The corresponding excitation energy, 4.72 eV at the CP geometry, is thus clearly out of the wavelength domain of interest (it would transfer into 263 nm while one seeks there at explaining a maximum of absorption at 418 nm). Once the SOC is introduced, the triply degenerate spin-triplet SOF state is split into three components, one of which being mixed with the triply degenerate spin-singlet components (see Figure 3). Because of this mixing arising at the second order of perturbations, two electronic transitions are then active (red arrows in Figure 3), leading to two transitions with non-zero oscillator strengths (see Table 3). The "smallest" arrow, corresponding to an excitation energy of 3.01 eV, would transfer into 412 nm, while the "longest" one, corresponding to 5.30 eV, would transfer into 234 nm (see Table S1). Clearly, it is thus crucial to include the SOC while computing the smallest excitation energies in these systems, in particular to obtain characteristic absorption wavelengths in the right domain (here, around 418 nm, within a few tenths of nm of margins). Note that in this complex, both the GP and CP geometries lead to similar excitation energies (and thus, anticipated maxima of absorption).

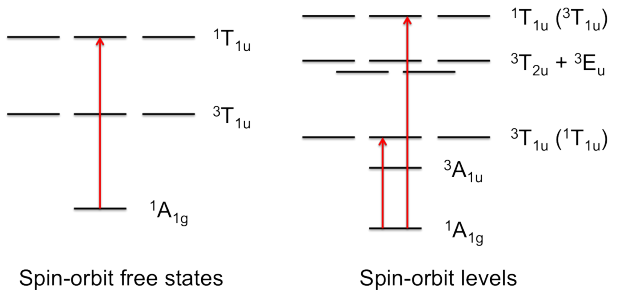

Figure 3: Ground and singly-excited spin-orbit free states and spin-orbit levels of the $[PoCl_6]^{2-}$ complex (O_h symmetry point group). Significant but not dominant components are given in parentheses. Spin-allowed transitions from the ground spin-orbit free and spin-orbit states are indicated by red arrows.

For the other two $[PoCl_{2+x}]^{2-x}$ candidates (x = 3, 2), the SOC also has an important role on the excitation energies (see Tables 2 and 3). According to our results, both the $[PoCl_5]^-$ and $PoCl_4$ complexes would display significant absorption properties above 468 nm, *i.e.* more than 50 nm above the targeted maximum of absorption. For these wavelengths, 50 nm would transfer into 0.32 eV. On the SOF excitation energies of interest, the effect of

Table 2: Gas-Phase NEVPT2 Excitation Energies (in eV) as Functions of the Geometry. The Numbers of Degenerate Components Are Given in Parentheses When Relevant.

		GP	
Species	Geometry	$\Delta E(S_0 \rightarrow T_{1-3})$	$\Delta E(S_0 \rightarrow S_{1-3})$
$[PoCl_6]^{2-}$	GP = O_h	4.23(3)	4.65(3)
	CP = O_h	4.30(3)	4.72(3)
$[PoCl_5]^-$	GP = D_{3h}	3.46(2); 4.38	3.86(2); 4.93
	CP = C_{4v}	3.09; 4.36(2)	3.29; 4.99(2)
$PoCl_4$	GP = C_{2v}	3.02; 3.28; 3.58	3.57; 3.79; 3.97
	CP = C_{2v}	3.20; 3.39; 4.41	3.35; 3.57; 5.49
$[Po(OH)Cl_4]^-$	GP = C_s	4.14; 4.45; 4.59	4.29; 5.03; 5.26
	CP = C_s	4.14; 4.51; 4.58	4.28; 5.12; 5.28
$Po(OH)Cl_3$	GP = C_1	3.65; 4.39; 4.51	3.90; 4.44; 5.69
	CP = C_1	3.64; 4.37; 4.47	3.83; 4.40; 5.71
$[Po(OH)Cl_2]^+$	GP = C_s	4.81; 5.75; 6.16	5.13; 6.01; 6.09
	CP = C_s	4.73; 5.64; 6.17	5.04; 5.95; 6.03

the C-PCM that is missed in our WFT calculations is meant to be less than 0.2 eV (at the TD-DFT level). Since the SOC is then mixing the spin-singlet SOF states with some of the spin-triplet components, we anticipate that the bias that we introduce by not considering the C-PCM perturbation is actually less important than the error that is done on one given excitation energy. As a consequence, we believe that the results reported in Table 3 are accurate enough to make a distinction between all the considered $[PoCl_{2+x}]^{2-x}$ candidates (x = 4–2), meaning that our calculations are in favor of the occurrence of the $[PoCl_6]^{2-}$ complex for HCl concentrations above 0.5M.

Out of the analysis of Moyer,[11] to a given $[PoCl_{2+x}]^{2-x}$ complex was meant to correspond a $[Po(OH)Cl_x]^{3-x}$ one. If one assumes that the conclusion of the previous paragraph is correct, then this complex must be the $[Po(OH)Cl_4]^-$ one. Thus, a further important discussion, for consistency with the analysis of Moyer, relates to the spectrum of this complex, and in particular, if it is compatible with a maximum of absorption at 344 nm. According to Tables 3 and S1, it is indeed the case (a maximum of absorption is for instance predicted around 355 nm). Therefore, according to our calculations, the occurence of the $[Po(OH)Cl_4]^-$ complex at low HCl concentration is compatible with the data of Moyer.

A last point worth being discussed concerns the potential occurrence of the other

Table 3: Gas-Phase c-SOCI Excitation Energies (in eV) as Functions of the Geometry. The Numbers of Degenerate Components, When Relevant, and the Oscillator Strengths Are Given in Parentheses for Facile Identification of the Allowed/Forbidden Transitions.

		GP			
Species	Geometry	ΔE_1	ΔE_2	ΔE_3	ΔE_4
$[PoCl_6]^{2-}$	GP = O_h	2.82 (0.000)	2.94 (3, 0.083)	4.94 (5, 0.000)	5.23 (3, 0.431)
	CP = O_h	2.88 (0.000)	3.01 (3, 0.084)	5.03 (5, 0.000)	5.30 (3, 0.434)
$[PoCl_5]^-$	GP = D_{3h}	2.42 (0.000)	2.50 (0.043)	2.56 (2, 0.060)	4.08 (0.000)
	CP = C_{4v}	2.52 (0.000)	2.60 (2, 0.038)	2.65 (0.031)	4.28 (0.000)
$PoCl_4$	GP = C_{2v}	2.11 (0.000)	2.19 (0.023)	2.25 (0.037)	2.31 (0.065)
	CP = C_{2v}	2.51 (0.000)	2.57 (0.013)	2.60 (0.011)	2.63 (0.041)
$[Po(OH)Cl_4]^-$	GP = C_s	3.28 (0.000)	3.35 (0.014)	3.39 (0.057)	3.48 (0.111)
	CP = C_s	3.31 (0.000)	3.38 (0.012)	3.45 (0.070)	3.50 (0.103)
$Po(OH)Cl_3$	GP = C_1	3.11 (0.000)	3.15 (0.004)	3.27 (0.037)	3.28 (0.060)
	CP = C_1	3.10 (0.000)	3.13 (0.003)	3.21 (0.026)	3.28 (0.060)
$[Po(OH)Cl_2]^+$	GP = C_s	4.32 (0.009)	4.34 (0.000)	4.39 (0.030)	4.57 (0.023)
	CP = C_s	4.24 (0.003)	4.26 (0.000)	4.33 (0.033)	4.48 (0.019)

$[PoCl_{2+x}]^{2-x}$ complexes, namely $Po(OH)Cl_3$ and $[Po(OH)Cl_2]^+$, at low HCl concentration. While $[Po(OH)Cl_2]^+$ seems excluded (no predicted characteristic absorption wavelength above 300 nm in Table S1), it is hard to discard the $Po(OH)Cl_3$ one based on this comparison between theory and experiment. Indeed, our calculations indicate a maximum of absorption above 344 nm, associated with a smaller oscillator strength than the one predicted for the $[Po(OH)Cl_4]^-$ complex (though this indicator should not be seen as a truly quantitative one). Therefore, one cannot firmly exclude the possibility for forming this species, and this species to be quite hidden in the spectrum because of the occurence of the $[Po(OH)Cl_4]^-$ one. Although no sign for this appears in the reported data[11] (for instance no "shoulder" has been observed), we believe that further experimental and/or theoretical studies are still required to elucidate the speciation of polonium(IV) in HCl medium. In particular, we plan to perform X-ray absorption spectroscopy experiments in a near future, which should provide us with more "direct" structural information from the experiment. It will be especially important to check for the presence of water molecules in the immediate environment of the polonium(IV) ion for the hydroxo complex(es) of interest (namely $[Po(OH)Cl_4]^-$, and perhaps also $Po(OH)Cl_3$). For the $[PoCl_6]^{2-}$ complex, we believe that the size of the chloride ions

should prevent such a presence, such that it should be possible to explain the experimental data without involving an O atom in the first coordination sphere of the polonium(IV) ion, as was observed for the isoelectronic $[BiCl_6]^{3-}$ complex.[54] If applicable, a quantum chemical study for which water molecules are explicitly treated will be particularly indicated for going beyond the fully-implicit C-PCM picture.

4 Concluding Remarks

In this work, we have revisited the UV-Vis spectroscopy of polonium(IV) chloride complexes in HCl medium by means of relativistic *and* multiconfigurational calculations. To the best of our knowledge, this constitutes the first electronic structure study of this kind dedicated to polonium species of actual experimental interest in solution. Although we are aware that more systematic methodological studies are still required, for instance regarding the implicit solvation model parameters (*e.g.* atomic radii), the explicit quantum chemical treatment of water molecules, the choice of the exchange-correlation functional (DFT), basis set (DFT and WFT), active space (WFT) and so on, this first study has already allowed us to reach two main conclusions: (i) it is crucial to account for the SOC while computing excitation energies of polonium(IV) complexes, although it is not necessary for computing the molecular geometries and (ii) the species discussed by Moyer and observed several decades ago[11] are most probably $[Po(OH)Cl_4]^-$ (for low HCl concentration) and $[PoCl_6]^{2-}$ (for HCl concentrations above 0.5M). For this latter situation, several indirect experimental studies have also reached a similar conclusion,[12–16] meaning that we are quite confident in being capable of characterizing it in a forthcoming experimental study.

Supporting Information Available

Gas-phase c-SOCI absorption wavelengths and atomic coordinates of the gas-phase and condensed-phase geometrical structures of the $[PoCl_{2+x}]^{2-x}$ and $[Po(OH)Cl_x]^{3-x}$ complexes.

Acknowledgment

This work was performed using high-performance computing resources from CCIPL ("Centre de Calcul Intensif des Pays de la Loire") and supported by the Pollusols program funded by the *Région des Pays de la Loire*.

References

(1) Ansoborlo, E.; Berard, P.; Den Auwer, C.; Leget, R.; Menetrier, F.; Younes, A.; Montavon, G.; Moisy, P. Review of Chemical and Radiotoxicological Properties of Polonium for Internal Contamination Purposes. *Chem. Res. Toxicol.* **2012**, *25*, 1551–1564.

(2) Ansoborlo, E. Poisonous Polonium. *Nat. Chem.* **2014**, *6*, 454.

(3) Persson, B. R.; Holm, E. Polonium-210 and Lead-210 in the Terrestrial Environment: A Historical Review. *J. Environ. Radioact.* **2011**, *102*, 420–429.

(4) Muggli, M. E.; Ebbert, J. O.; Robertson, C.; Hurt, R. D. Waking a Sleeping Giant: The Tobacco Industry's Response to the Polonium-210 Issue. *Am. J. Public Health* **2008**, *98*, 1643–1650.

(5) Sahu, S.; Tiwari, M.; Bhangare, R.; Pandit, G. Enrichment and Particle Size Dependence of Polonium and Other Naturally Occurring Radionuclides in Coal Ash. *J. Environ. Radioact.* **2014**, *138*, 421–426.

(6) Charles, G. W. Spectra of ^{208}Po and the Hyperfine Structure of ^{209}Po*. *J. Opt. Soc. Am.* **1966**, *56*, 1292–1297.

(7) Raeder, S.; Heggen, H.; Teigelhöfer, A.; Lassen, J. Determination of the First Ionization Energy of Polonium by Resonance Ionization Spectroscopy – Part I: Measurement of Even-Parity Rydberg States at TRIUMF-ISAC. *Spectrochim. Acta B* **2018**, *151*, 65–71.

(8) Fink, D.; Blaum, K.; Fedosseev, V.; Marsh, B.; Rossel, R.; Rothe, S. Determination of the First Ionization Energy of Polonium by Resonance Ionization Spectroscopy – Part II: Measurement of Odd-Parity Rydberg States at CERN—ISOLDE. *Spectrochim. Acta B* **2018**, *151*, 72–82.

(9) Borschevsky, A.; Pašteka, L. F.; Pershina, V.; Eliav, E.; Kaldor, U. Ionization Potentials and Electron Affinities of the Superheavy Elements 115–117 and Their Sixth-Row Homologues Bi, Po, and At. *Phys. Rev. A* **2015**, *91*, 020501.

(10) Younes, A.; Montavon, G.; Gouin, S. G.; André-Joyaux, E.; Peumery, R.; Chalopin, T.; Alliot, C.; Mokili, M.; Champion, J.; Deniaud, D. Investigation of a New "$N_2S_2O_2$" Chelating Agent with High Po(IV) Affinity. *Chem. Commun.* **2017**, *53*, 6492–6495.

(11) Moyer, H. V. In *Polonium*; Moyer, H. V., Ed.; United States Atomic Energy Commission: Oak Ridge, Tenessee, 1956; Chapter 4, pp 33–96.

(12) Bagnall, K. W.; Freeman, J. H. 544. Electrochemical Studies on Polonium. *J. Chem. Soc.* **1956**, 2770–2774.

(13) Danon, J.; Zamith, A. A. L. Ion-Exchange and Solvent-Extraction Studies with Polonium. *J. Phys. Chem.* **1957**, *61*, 431–434.

(14) Sheppard, J.; Warnock, R. The Distribution of Bismuth (III) and Polonium (IV) Between Trilaurylamine Solutions of Xylene and Hydrochloric and Hydrobromic Acid Solutions. *J. Inorg. Nucl. Chem.* **1964**, *26*, 1421–1427.

(15) Marcus, Y. Metal-Chloride Complexes Studied by Ion-Exchange and Solvent-Extraction Methods: Part I. Non-Transition-Metal Ions, Lanthanides, Actinides, and d^0 Transition-Metal Ions. *Coord. Chem. Rev.* **1967**, *2*, 195–238.

(16) Younes, A.; Alliot, C.; Mokili, B.; Deniaud, D.; Montavon, G.; Champion, J. Solvent

Extraction of Polonium(IV) with Tributylphosphate (TBP). *Solvent Extr. Ion Exc.* **2017**, *35*, 77–90.

(17) Cossi, M.; Rega, N.; Scalmani, G.; Barone, V. Energies, Structures, and Electronic Properties of Molecules in Solution with the C-PCM Solvation Model. *J. Comput. Chem.* **2002**, *24*, 669–681.

(18) Angeli, C.; Cimiraglia, R.; Malrieu, J.-P. *N*-Electron Valence State Perturbation Theory: A Fast Implementation of The Strongly Contracted Variant. *Chem. Phys. Lett.* **2001**, *350*, 297–305.

(19) Rota, J.-B.; Knecht, S.; Fleig, T.; Ganyushin, D.; Saue, T.; Neese, F.; Bolvin, H. Zero Field Splitting of the Chalgogen Diatomics Using Relativistic Correlated Wave-Function Methods. *J. Chem. Phys.* **2011**, *135*, 114106.

(20) Gomes, A. S. P.; Réal, F.; Galland, N.; Angeli, C.; Cimiraglia, R.; Vallet, V. Electronic Structure Investigation of the Evanescent AtO^+ Ion. *Phys. Chem. Chem. Phys.* **2014**, *16*, 9238–9248.

(21) Maurice, R.; Réal, F.; Gomes, A. S. P.; Vallet, V.; Montavon, G.; Galland, N. Effective Bond Orders from Two-Step Spin-Orbit Coupling Approaches: The I_2, At_2, IO^+, and AtO^+ Case Studies. *J. Chem. Phys.* **2015**, *142*, 094305.

(22) Sergentu, D.-C.; Amaouch, M.; Pilmé, J.; Galland, N.; Maurice, R. Electronic Structures and Geometries of the XF_3 (X = Cl, Br, I, At) Fluorides. *J. Chem. Phys.* **2015**, *143*, 114306.

(23) Sergentu, D.-C.; Réal, F.; Montavon, G.; Galland, N.; Maurice, R. Unraveling the Hydration-Induced Ground-State Change of AtO^+ by Relativistic and Multiconfigurational Wave-Function-Based Methods. *Phys. Chem. Chem. Phys.* **2016**, *18*, 32703–32712.

(24) Vallet, V.; Maron, L.; Teichteil, C.; Flament, J.-P. A Two-Step Uncontracted Determinantal Effective Hamiltonian-Based SO–CI Method. *J. Chem. Phys.* **2000**, *113*, 1391–1402.

(25) M. J. Frisch, G. W. Trucks, H. B. Schlegel, G. E. Scuseria, M. A. Robb, J. R. Cheeseman, G. Scalmani, V. Barone, B. Mennucci, G. A. Petersson, et al.; Gaussian 09, Revision D.01 (2009), Gaussian, Inc., Wallingford CT.

(26) Lee, C.; Yang, W.; Parr, R. G. Development of the Colle-Salvetti Correlation-Energy Formula into a Functional of the Electron Density. *Phys. Rev. B* **1988**, *37*, 785–789.

(27) Becke, A. D. Density Functional Thermochemistry. III. The Role of Exact Exchange. *J. Chem. Phys.* **1993**, *98*, 5648–5652.

(28) Stephens, P. J.; Devlin, F. J.; Chabalowski, C. F.; Frisch, M. J. Ab Initio Calculation of Vibrational Absorption and Circular Dichroism Spectra Using Density Functional Force Fields. *J. Phys. Chem.* **1994**, *98*, 11623–11627.

(29) Dunning Jr., T. H. Gaussian Basis Sets for Use in Correlated Molecular Calculations. I. The Atoms Boron through Neon and Hydrogen. *J. Chem. Phys.* **1989**, *90*, 1007–1023.

(30) Kendall, R. A.; Dunning, T. H.; Harrison, R. J. Electron Affinities of The First Row Atoms Revisited. Systematic Basis Sets and Wave Functions. *J. Chem. Phys.* **1992**, *96*, 6796–6806.

(31) Woon, D. E.; Dunning, T. H. Gaussian Basis Sets for Use in Correlated Molecular Calculations. III. The Atoms Aluminum Through Argon. *J. Chem. Phys.* **1993**, *98*, 1358–1371.

(32) Peterson, K. A.; Figgen, D.; Goll, E.; Stoll, H.; Dolg, M. Systematically Convergent Basis Sets With Relativistic Pseudopotentials. II. Small-Core Pseudopotentials and

Correlation Consistent Basis Sets For The Post-d Group 16–18 Elements. *J. Chem. Phys.* **2003**, *119*, 11113–11123.

(33) Ayala, R.; Martinez, J. M.; Pappalardo, R. R.; Muñoz Paez, A.; Sanchez Marcos, E. Po(IV) hydration: A Quantum Chemical Study. *J. Phys. Chem. B* **2008**, *112*, 5416–5422.

(34) Rappé, A. K.; Casewit, C. J.; Colwell, K. S.; Goddard III, W. A.; Skiff, W. M. UFF, a Full Periodic Table Force Field for Molecular Mechanics and Molecular Dynamics Simulations. *J. Am. Chem. Soc.* **1992**, *114*, 10024–10035.

(35) Ayala, R.; Martinez, J. M.; Pappalardo, R. R.; Muñoz Paez, A.; Sanchez Marcos, E. General Quantum-Mechanical Study of the Hydrolysis Equilibria for a Tetravalent Aquaion: The Extreme Case of the Po(IV) in Water. *J. Phys. Chem. B* **2009**, *113*, 487–496.

(36) Ayala, R.; Spezia, R.; Vuilleumier, R.; Martinez, J. M.; Pappalardo, R. R.; Sanchez Marcos, E. An Ab Initio Molecular Dynamics Study on the Hydrolysis of the Po(IV) Aquaion in Water. *J. Phys. Chem. B* **2010**, *114*, 12866–12874.

(37) Ayala, R.; Martinez, J. M.; Pappalardo, R. R.; Sanchez Marcos, E. Quantum-Mechanical Study on the Aquaions and Hydrolyzed Species of Po(IV), Te(IV), and Bi(III) in Water. *J. Phys. Chem. B* **2012**, *116*, 14903–14914.

(38) Barone, V.; Cossi, M.; Tomasi, J. A New Definition of Cavities for the Computation of Solvation Free Energies by the Polarizable Continuum Model. *J. Chem. Phys.* **1997**, *107*, 3210–3221.

(39) Runge, E.; Gross, E. K. U. Density-Functional Theory for Time-Dependent Systems. *Phys. Rev. Lett.* **1984**, *52*, 997–1000.

(40) F. Neese; ORCA – An Ab Initio, Density Functional and Semiempirical Program Package

(2014), version 3.0.3. Max-Planck-Institut für Bioanorganische Chemie, Mülheim an der Ruhr.

(41) Roos, B. O.; Taylor, P. R.; Siegbahn, P. E. M. A Complete Active Space SCF Method (CASSCF) Using a Density Matrix Formulated Super-CI Approach. *Chem. Phys.* **1980**, *48*, 157–173.

(42) Roos, B. O. In *Theory and Applications of Computational Chemistry: The First Forty Years*; Dykstra, C. E., Frenking, G., Kim, K. S., Scuseria, G. E., Eds.; Elsevier: Amsterdam, 2005; Chapter 25, pp 725–764.

(43) Dyall, K. G. The Choice of Zeroth-Order Hamiltonian for Second-Order Perturbation Theory with a Complete Active Space Self-Consistent-Field Reference Function. *J. Chem. Phys.* **1995**, *102*, 4909–4918.

(44) Teichteil, C.; Pélissier, M.; Spiegelmann, F. Ab Initio Molecular Calculations Including Spin-Orbit Coupling. I. Method and Atomic Tests. *Chem. Phys.* **1983**, *81*, 273–282.

(45) Llusar, R.; Casarrubios, M.; Barandiarán, Z.; Seijo, L. Ab Initio Model Potential Calculations on the Electronic Spectrum of Ni^{2+} Doped MgO Including Correlation, Spin-Orbit and Embedding Effects. *J. Chem. Phys.* **1996**, *105*, 5321–5330.

(46) Douglas, M.; Kroll, N. M. Quantum Electrodynamical Corrections to The Fine Structure of Helium. *Ann. Phys.* **1974**, *82*, 89–155.

(47) Hess, B. A. Relativistic Electronic-Structure Calculations Employing a Two-Component No-Pair Formalism With External-Field Projection Operators. *Phys. Rev. A* **1986**, *33*, 3742–3748.

(48) Jansen, G.; Hess, B. A. Revision of the Douglas-Kroll Transformation. *Phys. Rev. A* **1989**, *39*, 6016–6017.

(49) Hess, B. A.; Marian, C. M.; Wahlgren, U.; Gropen, O. A Mean-Field Spin-Orbit Method Applicable to Correlated Wavefunctions. *Chem. Phys. Lett.* **1996**, *251*, 365–371.

(50) Neese, F. Efficient and Accurate Approximations to the Molecular Spin-Orbit Coupling Operator and their Use in Molecular g-Tensor Calculations. *J. Chem. Phys.* **2005**, *122*, 034107.

(51) Pantazis, D. A.; Chen, X.-Y.; Landis, C. R.; Neese, F. All-Electron Scalar Relativistic Basis Sets for Third-Row Transition Metal Atoms. *J. Chem. Theory Comput.* **2008**, *4*, 908–919.

(52) Pantazis, D. A.; Neese, F. All-Electron Scalar Relativistic Basis Sets for The 6p Elements. *Theor. Chem. Acc.* **2012**, *131*, 1292–1299.

(53) Bersuker, I. B. Pseudo-Jahn–Teller Effect—A Two-State Paradigm in Formation, Deformation, and Transformation of Molecular Systems and Solids. *Chem. Rev.* **2013**, *113*, 1351–1390.

(54) Etschmann, B. E.; Liu, W.; Pring, A.; Grundler, P. V.; Tooth, B.; Borg, S.; Testemale, D.; Brewe, D.; Brugger, J. The role of Te(IV) and Bi(III) chloride complexes in hydrothermal mass transfer: An X-ray absorption spectroscopic study. *Chem. Geol.* **2016**, *425*, 37–51.

Table of contents:

Artwork:

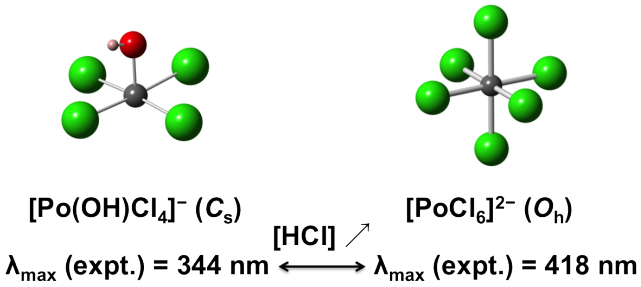

Synopsis:

In this work, we revisit the absorption properties of potentially occurring polonium(IV) complexes in HCl medium by confronting our computational results to old experimental ones, concluding that at least two complexes are susceptible to occur, $[Po(OH)Cl_4]^-$ (low HCl concentration) and $[PoCl_6]^{2-}$ (HCl concentrations above 0.5M). Moreover, we show that solvation can remarkably change the polonium(IV) molecular geometries, and that the SOC must be here accounted for in the calculation to obtain correct excitation energies.